

Effect of Threshold Voltage on Field-Effect Transistor and Phototransistor Performance Based on Pentacene

Bushra H. Mohammed*^{1a} and Noora H. Ali^{1b}

¹ Department of Physics, College of Science, University of Thi-Qar, Nasiriya 64001, Iraq.

^bE-mail: noorafofo33@sci.utq.edu.iq,

^{a*} Corresponding author: bushra.hussain_ph@sci.utq.edu.iq

Received: 2025-10-02, Revised: 2025-11-28, Accepted: 2025-12-13, Published: 2026-06-01

Abstract— This study shows that the suggested model greatly improves the OFET-based photodetector's performance for the organic semiconductor pentacene and the dielectric polyvinyl alcohol (PVA). This model shows how the threshold voltage affects both types' electrical characteristics (the output and transfer). Various incident optical power (P_{opt}) values between 100 and 1000 $\mu\text{W}/\text{cm}^2$ were tested. The results show that the threshold voltage exhibits nonlinear behaviour, rising as incident optical power increases. Where MATLAB software simulation is used to calculate the electrical properties output (I_d - V_d) and transfer (I_d - V_g) properties, including current (I_d) values, switching ratio (I_{on}/I_{off}), and responsivity (R). Pentacene exhibits transfer and output properties typical of p-type OFETs. The ideal drain current value for output (I_d - V_d) and transfer (I_d - V_g) properties is found at an incident optical power of $P_{opt} = 1000 \mu\text{W}/\text{cm}^2$, a threshold voltage of $V_{th} = -0.63 \text{ V}$, and a gate voltage of $V_g = -30 \text{ V}$. While the responsivity shows the opposite behavior, the observed switching ratio values increase as the threshold voltage and incident optical power decrease. The OFET-based photodetector functioned best at the lowest threshold voltage value of -0.63 V . This decrease in threshold voltage (V_{th}) is critical for OFET-based electronic applications because it boosts photocurrent and enhances responsiveness R .

Keywords— organic field-effect transistor OFET, Threshold voltage V_{th} , phototransistor PT, Pentacene, Photosensitivity P.

I. INTRODUCTION

Inorganic semiconductors, due to their rigid structure, are not promising for wearable, flexible phototransistors in home-assisted or clinical sensor applications because their expensive production conditions make them unsuitable for high-throughput, cost-effective technologies [1-6]. Organic semiconductor materials, which include small molecules and polymers, have made it possible to create new opportunities to overcome the defects found in inorganic semiconductor materials [7-9]. Organic semiconductor devices have attracted significant attention since they have revealed mechanically flexible, inexpensive, low-power, soft, non-invasive light optoelectronic devices for both industrial and clinical purposes [10].

Thus, it defines that a particular kind of photodetector called a phototransistor (PT) converts an

incident light signal into an electrical signal that can be detected. The unique three-electrode design of a phototransistor, for example, enhances the signal and lowers noise, giving this device better functionality than other photodetector devices, such as photodiodes, where numerous sectors, including medical applications, optical communications, industrial and environmental studies, disaster weather prediction, digital imaging, logic gates, and fire warning, have made use of phototransistors [2, 11-13].

Among these organic semiconductors was the Pentacene molecule, which is one of the most studied organic semiconductor materials, P-type, characterized by high air stability, high switching ratio (I_{on}/I_{off}), and high carrier mobility, exhibiting high electrical and photosensitive properties. In addition, organic phototransistors (OPTs) use pentacene material because of its strong electrical performance and absorbent properties, which result in a higher generation efficiency across a wide wavelength range [14-17]. Depending on the photon energy, a pentacene-based transistor can exhibit different behaviors when excited by light. It has been shown that when the illumination intensity is increased, the saturation current strengthens, the threshold voltage (V_{th}) shifts positively, and the total trap density decreases under white or low-energy ultraviolet (UV) light. An excellent option for the active layer in an organic photodetector with a FET architecture is the pentacene material [18-19].

Polyvinyl alcohol (PVA) is one of the most common polymer dielectrics, which can provide a low-trap-density surface and a smooth surface. PVA agrees with organic semiconductor materials [20-21].

This research aims to study the effect of the threshold voltage (V_{th}) on the electrical properties of both types (the output and transfer) for the FET-based organic photodetectors (OPTs), and by using different values for the incident optical power (P_{opt}) for the organic semiconductor (Pentacene) and the insulator PVA.



II. THEORETICAL MODEL

For the dependence of the threshold voltage (V_{th}) parameters on the present illumination, the threshold voltage (V_{th}) can be accounted for by the following equation [22]:

$$\Delta V_{th} = \frac{AKT}{G_M q} \ln \left(1 + \frac{\eta q \lambda p_{opt}}{I_{pd} h c} \right) \quad (1)$$

where G_M is the transconductance, q is the electronic charge, p_{opt} is the incident optical power, η is the quantum efficiency, hc/λ is the photon energy, I_{pd} is the dark current for electrons, V_{th} is the threshold voltage shift, and A is the fitting parameter.

Eq. 1 indicates that the coefficients in the magnitude $(1 + \frac{\eta q \lambda p_{opt}}{I_{pd} h c})$ do not influence the calculation of the threshold voltage, as the number 1 is significantly larger than the magnitude $(\frac{\eta q \lambda p_{opt}}{I_{pd} h c})$, which is itself very small relative to 1. Thus, these coefficients have minimal impact on the threshold voltage. Consequently, it is essential to derive an equation in which these coefficients play a role in calculating the threshold voltage (V_{th}):

$$\Delta V_{th} = \frac{AKT}{G_M} \ln \left(\frac{\eta \lambda p_{opt}}{I_{pd} h c} \right) \quad (2)$$

Moreover, FET-based organic photodetectors have one of the main detecting parameters that determine the realization of photodetectors, namely, responsivity (R). To quantify the photoresponse performance of PTs, the responsivity (R) of a photodetector is an essential metric that measures how effectively it transforms incoming light into an electrical signal. In the case of organic field-effect transistors (OFETs), responsivity (R) is defined as the ratio of the photocurrent produced by the device to the incident optical power, as represented by the following equation. [23- 27]:

$$R = \frac{I_{ph}}{PA} \quad (3)$$

Where A is the area exposed to light.

The gradual-channel approximation model can be applied to calculate the current (I_d) flowing across the channel and to find the OFET operating parameters of the critical phototransistor. Phototransistors with OFETs can operate in two regions (the linear and saturation regions), in the saturation region given by [21- 28]:

$$I_d = \frac{WC_i}{2L} \mu \times \left[(V_g - V_{th})^2 \right] \quad (4)$$

We substitute Eq. (2) into Eq. (4), the current drain in the saturation region becomes:

$$I_d = \frac{WC_i}{2L} \mu \times \left[\left(V_g - \frac{AKT}{G_M} \ln \left(\frac{\eta \lambda p_{opt}}{I_{pd} h c} \right) \right)^2 \right] \quad (5)$$

$$I_d = \frac{WC_i}{L} \mu \times \left[(V_g - V_{th}) \times V_d - \frac{V_d^2}{2} \right] \quad (6)$$

We substitute Eq. (2) into Eq. (6). In the linear region, the drain current can be written as:

$$I_d = \frac{WC_i}{L} \mu \times \left[\left(V_g - \frac{AKT}{G_M} \ln \left(\frac{\eta \lambda p_{opt}}{I_{pd} h c} \right) \right) \times V_d - \frac{V_d^2}{2} \right] \quad (7)$$

The switching ratio can be measured by the following equation:

$$\frac{I_{on}}{I_{off}} = \frac{\mu \times ci \left(V_g - \frac{AKT}{G_M} \ln \left(\frac{\eta \lambda p_{opt}}{I_{pd} h c} \right) \right)^2}{2vd \times t \times gm} \quad (8)$$

Where W is the channel width, L is the channel length, μ is mobility in the linear region, the gate voltage is V_g , drain voltage V_d , and C_i is the gate insulator's and semiconductor's capacitance per unit area, where C_i can be written as[29-30]:

$$C_i = C_{dielectric} + C_{semiconductor}$$

$$C_i = \left(\frac{\epsilon_0 \epsilon_{dielectric}}{t_{dielectric}} \right) + \left(\frac{\epsilon_0 \epsilon_{semiconductor}}{t_{semiconductor}} \right) \quad (9)$$

MATLAB software was employed to determine V_{th} and (I-V) characteristics for the phototransistor in this model.

The structure of an OFET-based organic photodetector is designed in this study. The gate is indium tin oxide (ITO). The gate dielectric material is polyvinyl alcohol (PVA). The organic semiconductor (OS) is pentacene (P) with gold (Au) electrodes for the source and drain.

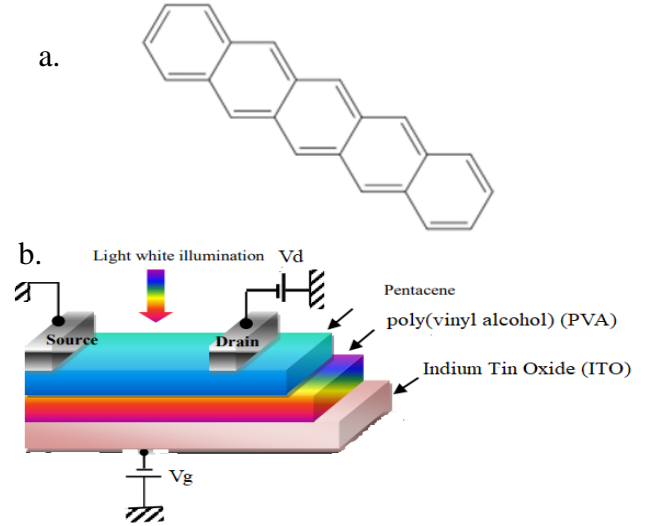


Fig. 1: (a) Molecular structure diagram of the pentacene [5] and (b) Schematic diagram of the Pentacene phototransistor structure.

III. RESULTS AND DISCUSSION

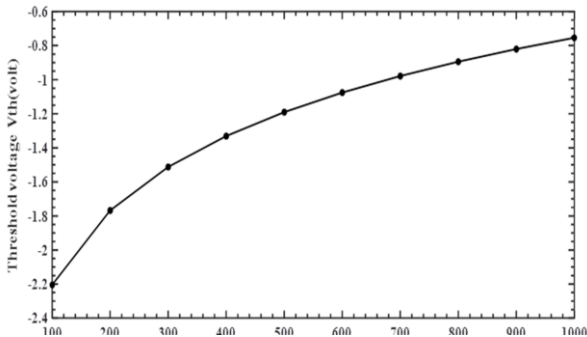
In this study, the influence of the threshold voltage V_{th} on FET-based organic photodetectors OPTs of the organic semiconductor of p-type Pentacene and a gate dielectric material (PVA) is studied. The study used different values of the incident optical power ($P_{opt}=100-1000 \mu W/(cm^2)$). The threshold voltage V_{th} is measured using Eq. (2) and using the parameter values shown in Table 1.

TABLE 1: the parameters used in this work.

Parameter	Value
area exposed to light A	$4 \times 10^{-4} \text{m}^2$
transconductance G_M	8.3×10^{-6}
Temperature T	350 K
quantum efficiency η	2×10^7
dark current I_{pd}	$2.5 \times 10^{-6} \text{A}$

The measured threshold voltage V_{th} shift on the same device is plotted against incident optical power, as shown in Figure 2. This figure shows nonlinear behavior for threshold voltage through an increase in the threshold voltage with increasing power, where the value for threshold voltage V_{th} is -0.63V at incident optical power ($P_{opt} = 1000 \mu\text{W}/\text{cm}^2$), while the value for threshold voltage V_{th} is -2.1 V at incident optical power ($P_{opt} = 100 \mu\text{W}/\text{cm}^2$). Reduced photosensitivity is due to the outcome of this nonlinear behaviour at higher light intensities, which goes back to the slow transfer of accumulated charges at the dielectric layer (PVA)/ organic semiconductor (Pentacene) interface. A proposed theoretical model expresses the dependence of the threshold voltage V_{th} shift parameters on illumination. The change in threshold voltage V_{th} values is due to the creation of carrier charges through visible light. Transistors must be incorporated into electrical circuitry. When visible light photons form positive dipoles at the organic semiconductor diode interface, they trap photogenerated holes at the transistor's dielectric layer/organic semiconductor (pentacene) interface, resulting in a negative gate voltage shift. This leads to a decrease in Threshold voltage (V_{th}) in Pentacene phototransistors (PT). Drop Threshold voltage (V_{th}) is necessary for electronic applications that utilize OFETs; this threshold voltage drop is crucial because it boosts light sensitivity but can also raise the "off-state" or dark current, making it more challenging to fully shut off the device. Increased photocurrent, enhanced responsiveness R and detectivity, and an increase in the minimum current flowing in the absence of light are the primary outcomes.

Fig. (2): Threshold voltage as a function of incident optical power of the Pentacene phototransistor.



Through investigating the effect of the threshold voltage V_{th} on the performance of the FET-based organic photodetector (PT), by using the proposed model, using different values

for the incident optical power ($P_{opt} = 100, 500, 1000 \mu\text{W}/\text{cm}^2$), and threshold voltage values ($V_{th} = -2.1, -1.1, \text{ and } -0.63 \text{ V}$) respectively. Where the electrical properties (output (I_d-V_d) and transfer properties (I_d-V_g)) of the Pentacene-based OFET are estimated using Eqs. (5) and (6), and using gate insulator PVA. These output properties (the linear and saturation regimes (I_d-V_d)) and transfer properties (the linear and saturation regimes (I_d-V_g)) are studied using the parameter values presented in Tables 1 and 2.

Figures 3 and 4 clearly illustrate the output and transfer characteristics of OFET-based pentacene photodetectors. As negative gate voltages V_g rise, Figures (3-4) show typical channel accumulation p-type OFET behaviour, revealing the linear and saturation areas of each device. The (drain-source current-drain voltage) (I_d-V_d) curves show good linearity at lower voltages. These demonstrate the formation of a strong ohmic contact between the Au and pentacene electrodes. These curves show how the source-drain current is obviously increased by the photocurrent contribution. Furthermore, similar to gate bias in OFETs, OPTs operate as a typical light-electric bi-functional device by utilizing incident light as an independent variable to modify transistor operation.

TABLE 2: PARAMETERS used in this work.

Parameter	Value
Width of channel W	$2.1 \times 10^{-6} \text{m}$
Length of channel L	$1 \times 10^{-6} \text{m}$
Semiconductor thickness ($t_{semiconductor}$)	1000 nm
Dielectric thickness ($t_{dielectric}$)	100nm
Mobility μ	$5 \times 10^{-4} \text{m}^2/\text{V.s}$
The dielectric constant of pentacene ($\epsilon_{semiconductor}$)	4.4
The dielectric constant of poly(vinyl alcohol) (PVA) ($\epsilon_{dielectric}$)	4.5

Figure (3) shows the drain current I_d versus the drain-source voltage ($V_d = -30$ to 0 V) for different gate-source voltage ($V_g = -30, -20, -10, 0 \text{ V}$), the incident optical power ($P_{opt} = 100, 500, \text{ and } 1000 \mu\text{W}/\text{cm}^2$), and threshold voltage ($V_{th} = -2.1, -1.1, \text{ and } -0.63 \text{ V}$), respectively. When negative gate voltages (V_g) are applied, the current I_d flows from the source to the drain through the channel area. This device observes typical output curves of OFET-based photodetectors. These curves show that only holes collect at the Pentacene / (PVA) interface. These curves also show that increasing V reaches the maximum value, which is -30V. The change in the threshold voltage towards negative voltages causes a decrease in the current levels. This behavior is typical for p-type OFETs in the presence of traps at the Pentacene/ insulator (PVA) contact, where adequate ohmic contact between contact electrodes (Au) and Pentacene is indicated by output characteristics that differentiate between the linear, pinch-off, and saturation regimes, as we mentioned earlier, this outcome is consistent with other earlier studies [21, 28-31].

In Figure 3(a), the highest linear and saturation current values of the phototransistor are reached at gate voltage

($V_g = -30V$), the incident optical power ($P_{opt} = 100 \mu W/cm^2$), and threshold voltage ($V_{th} = -2.1V$) in OFETs are $I_{d(Linear)} = -2.35 \times 10^{-4}A$ and $I_{dsat.} = -2.37 \times 10^{-4}A$, respectively. The maximum linear and saturation current values of the phototransistor at gate voltage ($V_g = -30V$), the incident optical power ($P_{opt} = 500 \mu W/cm^2$), and threshold voltage ($V_{th} = -1.1V$), reached $I_{d(Linear)} = -2.21 \times 10^{-4}A$ and $I_{dsat.} = 2.22 \times 10^{-4}A$, as shown in Figure 3(b), the highest current linear and saturation values of phototransistor at gate voltage ($V_g = -30V$), the incident optical power ($P_{opt} = 1000 \mu W/cm^2$), and threshold voltage ($V_{th} = -0.63V$) can be reached to $I_{d(Linear)} = -2.11 \times 10^{-4}A$ and $I_{dsat.} = -2.15 \times 10^{-4}A$, as shown in Figure 3(c).

The best of the drain current results was obtained using the incident optical power value ($P_{opt} = 1000 \mu W/cm^2$) and threshold voltage ($V_{th} = -0.63V$), as shown in Figure 3(c). While the least current values can be obtained using the incident optical values ($P_{opt} = 500$ and $100 \mu W/cm^2$), and threshold voltage values ($V_{th} = -2.1$ and $-1.1V$) (as shown in Figures 3(a and b)), such behavior can be attributed to the effect of the effective threshold voltage.

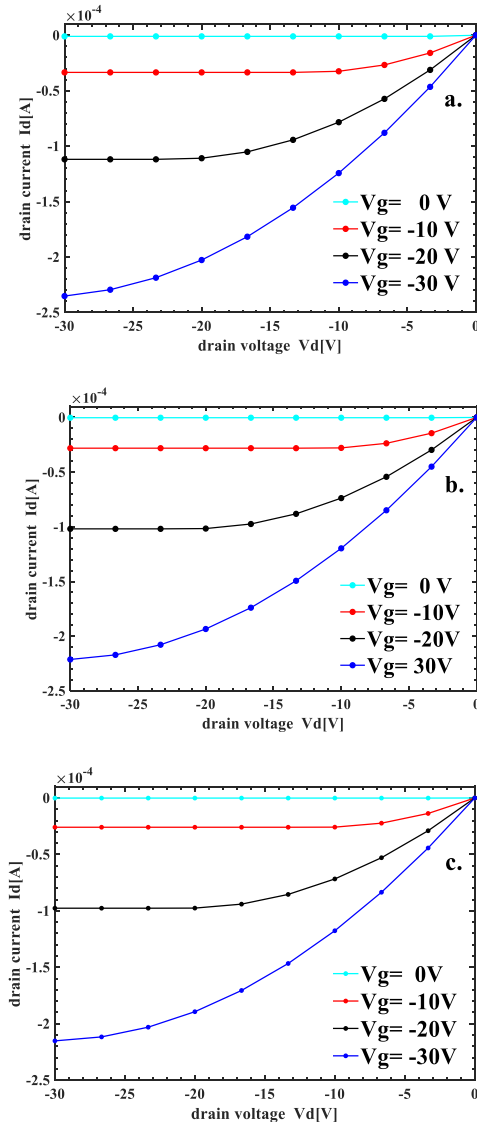


Fig. 3: Output characteristic (I_d-V_d) of the Pentacene (P) based OFET for gate insulator (PVA) at: (a) $P_{opt} = 100 \mu W/cm^2$ and $V_{th} = -2.1V$, (b) $P_{opt} = 500 \mu W/cm^2$ and $V_{th} = -1.1V$, and (c) $P_{opt} = 1000 \mu W/cm^2$ and $V_{th} = -0.63V$.

Figure 4 illustrates the transfer (I_d-V_g) characteristics of the Pentacene-based OFET phototransistor varying light intensities P_{opt} (100, 500, and $1000 \mu W/cm^2$) and threshold voltage ($V_{th} = -2.1, -1.1$, and $-0.63V$) with V_g from (-30 to $0V$) at $V_d = -30V$. Under light irradiation, the transfer curves (I_d-V_g) for each device show typical photoresponse behavior by shifting to the positive direction. The mobile electrons produced by the photon in the organic semiconductor would be captured if a positive gate bias were applied to the device while it was illuminated by light. It is possible to think of the electron traps as aiding in the formation of the transistor channel at a lower gate voltage by positively shifting the threshold voltage V_{th} . As a result, the current I_d will increase. The number of charges trapped can be further controlled by tuning the incident light intensity at a particular bias. Across different devices, as the incident optical power increases, the current (I_d) increases considerably. In Figure 4, the same behavior of output properties (I_d-V_d) curves is observed as in Figure 3. The highest value of the drain current is as in curve 4, at $V_g = -30V$. These results agree with the researchers' findings [21, 28-31].

However, as explained in Figure (4), the highest value of the linear and saturation drain current of the phototransistor (PT) for the incident optical power ($P_{opt} = 100 \mu W/cm^2$), and threshold voltage ($V_{th} = -2.1V$) in OFETs are $I_{d(Linear)} = -5.9 \times 10^{-4}A$ and $I_{dsat.} = -1.79 \times 10^{-4}A$ at $V_g = -30V$, respectively. While the maximum value of the linear and saturation drain current of the phototransistor (PT) for the incident optical power ($P_{opt} = 500 \mu W/cm^2$), and threshold voltage ($V_{th} = -1.1V$) are at $V_g = -30V$ $I_{d(Linear)} = -6.05 \times 10^{-4}A$ and $I_{dsat.} = -1.92 \times 10^{-4}A$. The highest values of the linear and saturation drain current are of the phototransistor (PT) for the incident optical power ($P_{opt} = 1000 \mu W/cm^2$), and threshold voltage ($V_{th} = -0.63V$) are $I_{d(Linear)} = -6.11 \times 10^{-4}A$ and $I_{dsat.} = -1.98 \times 10^{-4}A$ at $V_g = -30V$.

The best values of the (linear and saturation) drain current are obtained at the incident optical ($P_{opt} = 1000 \mu W/cm^2$) and threshold voltage ($V_{th} = -0.63V$) as shown in Figure 4. This behavior is due to the effective threshold voltage.

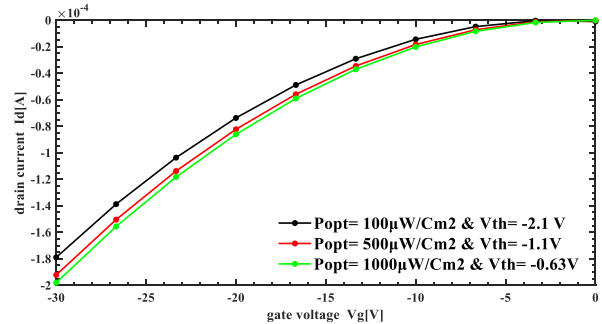


Fig. (4): Transfer characteristics (I_d-V_g) at drain voltage $-30V$ of the pentacene (p) based OFET for gate insulator (PVA).

Consequently, the best performance of the FET-based organic photodetector (PT) is at the minimum value of threshold voltage V_{th} , which is $-0.63V$, and an incident

optical power ($P_{\text{opt}} = 1000 \mu\text{W}/\text{cm}^2$) for both the output and transfer electrical properties.

The switching ratio ($I_{\text{on}}/I_{\text{off}}$) was calculated by using Eq. (8) for different values of the incident optical ($P_{\text{opt}} = 100, 500, \text{ and } 1000 \mu\text{W}/\text{cm}^2$), as shown in Table 3. The values of the ratio ($I_{\text{on}}/I_{\text{off}}$) of the Pentacene increased as the incident optical and threshold voltage decreased.

Responsivity (R) calculated for FET-based organic photodetectors (OPTs) by using Eq. (3) for different values of the incident optical power ($P_{\text{opt}} = 100, 500, \text{ and } 1000 \mu\text{W}/\text{cm}^2$), as observed in Table 3. The Responsivity R values of the PVA-Pentacene decreased with increasing incident optical power and threshold voltage.

Table 3: The $I_{\text{on}}/I_{\text{off}}$ ratios and responsivity (R) of pentacene for different values of the incident optical power P_{opt} .

V_{th} (V)	P_{opt} ($\mu\text{W}/\text{cm}^2$)	$I_{\text{on}}/I_{\text{off}}$	R (A/W)
-2.1	100	2×10^7	0.625
-1.1	500	1.88×10^7	0.125
-0.63	1000	1.83×10^7	0.00031

IV. CONCLUSIONS

This proposed model successfully improved the performance of the FET-based organic photodetector for organic semiconductor (Pentacene) and dielectric (PVA). The main conclusions are as follows: the study reveals the nonlinear behavior of the threshold voltage. The study also observes linear and saturation regions of the FET-based organic photodetector, clearly showing increasing negative gate voltages and exhibiting a typical channel accumulation p-type OFET behavior. The current values were increased at the highest value of the gate voltage $V_g = -30 \text{ V}$ for both output (I_d-V_d) and transfer (I_d-V_g) properties. The best values of the drain current (linear and saturation) are at threshold voltage ($V_{\text{th}} = -0.63 \text{ V}$) and the incident optical power ($P_{\text{opt}} = 1000 \mu\text{W}/\text{cm}^2$). The best performance of the OFET-based photodetector was at the minimum threshold voltage of -0.63 V . The switching ratio ($I_{\text{on}}/I_{\text{off}}$) values increase as the incident optical power and threshold voltage decrease. Conversely, the responsivity R values decrease with increasing incident optical power and threshold voltage.

FUNDING: No funding.

CONFLICT OF INTEREST

The authors declare that they have no conflict of interest.

REFERENCES

- [1] H. Xu, J. Liu, J. Zhang, G. Zhou, N. Luo, and N. Zhao, "Flexible organic/inorganic hybrid near-infrared photoplethysmogram sensor for cardiovascular monitoring," *Advanced Materials*, vol. 29, no. 31, p. 1700975, 2017.
- [2] C. Xie, C. K. Liu, H. L. Loi, and F. Yan, "Perovskite-based phototransistors and hybrid photodetectors," *Advanced Functional Materials*, vol. 30, no. 20, p. 1903907, 2020.
- [3] P. C. Chow and T. Someya, "Organic photodetectors for next-generation wearable electronics," *Advanced Materials*, vol. 32, no. 15, p. 1902045, 2020.
- [4] N. Li, Z. Lan, Y. S. Lau, J. Xie, D. Zhao, and F. Zhu, "SWIR photodetection and visualization realized by incorporating an organic SWIR sensitive bulk heterojunction," *Advanced Science*, vol. 7, no. 14, p. 2000444, 2020.
- [5] F. Li, J. Zhou, J. Zhang, and J. Zhao, "Research and Progress on Organic Semiconductor Power Devices", *Materials*, 17, 3362, 2024. 3362; <https://doi.org/10.3390/ma17133362>
- [6] A. Sarwar, Y. Wang, L. Conrad Winkler, T. Zhang, J. Schroder, D. Spoltore, K. Leo, and J. Benduhn, "Tailoring Hole-Blocking Layers Enables a Versatile Approach for Fast Photomultiplication-Type Organic Photodetectors", *Adv. Funct. Mater.*, 2424456, 2025. <https://doi.org/10.1002/adfm.202424456>
- [7] Y. H. Lee, M. Jang, M. Y. Lee, O. Y. Kweon, and J. H. Oh, "Flexible field-effect transistor-type sensors based on conjugated molecules," *Chem*, vol. 3, no. 5, pp. 724-763, 2017.
- [8] P. Gu, Y. Yao, L. Feng, S. Niu, and H. Dong, "Recent advances in polymer phototransistors," *Polymer Chemistry*, vol. 6, no. 46, pp. 7933-7944, 2015.
- [9] L. Dou, Y. Liu, Z. Hong, G. Li, and Y. Yang, "Low-bandgap near-IR conjugated polymers /molecules for organic electronics," *Chemical reviews*, vol. 115, no. 23, pp. 12633-12665, 2015.
- [10] M. Mas-Torrent, P. Hadley, N. Crivillers, J. Veciana, and C. Rovira, "Large photoresponsivity in high-mobility single-crystal organic field-effect phototransistors," *ChemPhysChem*, vol. 7, no. 1, pp. 86-88, 2006.
- [11] A. Tavasli, B. Gurunlu, D. Gunturkun, R. Isci, and S. Faraji, "A review on solution-processed organic phototransistors and their recent developments," *Electronics*, vol. 11, no. 3, p. 316, 2022.
- [12] Z. Wu, Y. Zhai, H. Kim, J. D. Azoulay, and T. N. Ng, "Emerging design and characterization guidelines for polymer-based infrared photodetectors," *Accounts of Chemical Research*, vol. 51, no. 12, pp. 3144-3153, 2018.
- [13] A. Prasoon, P. Dacha, H. Zhang, E. Unsal, M. Hamsch, A. Croy, Sh. Fu, N. Ngan Nguyen, K. Liu, H. Qi, S. Chung, M. Jeong, L. Gao, U. Kaiser, K. Cho, H. I. Wang, R. Dong, G. Cuniberti, M. Bonn, S. C. B. Mannsfeld, and X. Feng, "High-Performance Phototransistor Based on a 2D Polybenzimidazole Polymer", *Adv. Mater.*, 2505810, 2025.
- [14] A. El Amrani, B. Lucas, F. Hijazi, and A. Moliton, "Visible light effect on the performance of photocouplers/phototransistors based on pentacene," *Materials Science and Engineering: B*, vol. 147, no. 2-3, pp. 303-306, 2008.

- [15] C.-L. Fan, H.-Y. Tsao, Y.-S. Shiah, C.-W. Yao, and P.-W. Cheng, "Performance enhancement of pentacene-based organic thin-film transistors using a high-K PVA/low-K PVP bilayer as the gate insulator," *Polymers*, vol. 13, no. 22, p. 3941, 2021.
- [16] R. Liguori, W. C. Sheets, A. Facchetti, and A. Rubino, "Light-and bias-induced effects in pentacene-based thin film phototransistors with a photocurable polymer dielectric," *Organic Electronics*, vol. 28, pp. 147-154, 2016.
- [17] F. Yakuphanoglu and W. A. Farooq, "Flexible pentacene organic field-effect phototransistor," *Synthetic Metals*, vol. 161, no. 5-6, pp. 379-383, 2011.
- [18] B. Gunduz, O. A. Al-Hartomy, S. A. F. Al Said, A. A. Al-Ghamdi, and F. Yakuphanoglu, "Controlling of photoresponse properties of pentacene thin film phototransistors by dielectric layer thickness and channel widths," *Synthetic metals*, vol. 179, pp. 94-115, 2013.
- [19] H.-W. Zan, W.-W. Tsai, Y.-r. Lo, Y.-M. Wu, and Y.-S. Yang, "Pentacene-based organic thin film transistors for ammonia sensing," *IEEE Sensors Journal*, vol. 12, no. 3, pp. 594-601, 2011.
- [20] Y. J. Jeong, D. H. Kim, Y.-M. Kang, and T. K. An, "Overcoating BaTiO₃ dielectrics with a fluorinated polymer to produce highly reliable organic field-effect transistors," *Thin Solid Films*, vol. 685, pp. 40-46, 2019.
- [21] B. H. Mohammed and E. T. Abdullah, "Study the performance of pentacene based organic field effect transistor by using monolayer, bilayer and trilayer with different gate insulators," *Iraqi Journal of Physics*, vol. 18, no. 44, pp. 85-97, 2020.
- [22] H.-S. Kang, C.-S. Choi, W.-Y. Choi, D.-H. Kim, and K.-S. Seo, "Characterization of phototransistor internal gain in metamorphic high-electron-mobility transistors," *Applied physics letters*, vol. 84, no. 19, pp. 3780-3782, 2004.
- [23] Ş. Rüzgar and M. Çağlar, "The Electrical Properties of Fabricated Pentacene Based Phototransistor with Polystyrene Gate Insulator," *Bitlis Eren Üniversitesi Fen Bilimleri Dergisi*, vol. 9, no. 3, pp. 1031-1039, 2020.
- [24] D. Yang, L. Zhang, S. Yang, and B. Zou, "Influence of the dielectric PMMA layer on the detectivity of pentacene-based photodetector with field-effect transistor configuration in visible region," *IEEE Photonics Journal*, vol. 5, no. 6, pp. 6801709-6801709, 2013.
- [25] P. Giraud *et al.*, "Field effect transistors and phototransistors based upon p-type solution-processed PbS nanowires," *Nanotechnology*, vol. 29, no. 7, p. 075202, 2018.
- [26] J. H. Kim *et al.*, "Ultrasensitive Near-Infrared InAs Colloidal Quantum Dot-ZnON Hybrid Phototransistor Based on a Graded Band Structure," *Advanced Science*, vol. 10, no. 18, p. 2207526, 2023.
- [27] Ch. Li, and X. Ren, "Geometric Effect of the Photo Responsivity of Organic Phototransistors", *Materials*, 18, 3349, 2025.
- [28] B. H. Mohammed and E. T. Abdullah, "Comparison between horizontal and vertical OFETs by using poly (3-Hexylthiophene)(P₃HT) as an active semiconductor layer," *Iraqi Journal of Science*, pp. 1040-1050, 2020.
- [29] B. H. Mohammed and E. T. Abdullah, "Effect of the thickness of semiconductor on the performance vertical organic field effect transistor by using grain size model", *Applied Physics A*, Volume 131, number 706, (2025).
- [30] B. H. Mohammed and E. T. Abdullah, "Effect of Channel Length on the Performance of C60 Organic Field Effect Transistors Utilizing Grain Size Modeling", *Bas J Sci* 43(2), 449-463, (2025).
- [31] E. T. Abdullah and B. H. Mohammed, "Effects of Thicknesses of Two Different Gate Insulators on the Performance of Pentacene Based Organic Field Effect Transistor", *Basrah Journal of Science*, Vol. 39(1), 56-66, 2021.